Prestack imaging of overturned reflections by reverse time migration

Biondo Biondi and Guojian Shan, Stanford University

SUMMARY

We present a simple method for computing angle-domain Common Image Gathers (CIGs) using prestack reverse time migration. The proposed method is an extension of the method proposed by Rickett and Sava (2001) to compute CIGs by downward-continuation shot-profile migration. We demonstrate with a synthetic example the use of the CIG gathers for migration velocity updating. A challenge for imaging both overturned and prismatic reflections is the discrimination of the reflection generated on either side of interfaces. We show how the propagation direction of the reflections can be determined by evaluating the crosscorrelation of the source wavefield with the receiver wavefield at time lags different than zero. Reflections can be easily separated once their direction of propagation is determined. We demonstrate the method by imaging overturned events generated by a segment of dipping reflector immersed in a vertically layered medium. We also applied the method to a North Sea data set with overturned events. The results of reverse time prestack migration are superior to the one obtained by a downward-continuation migration, and the CIGs obtained by applying the proposed method provide useful information for velocity updating.

INTRODUCTION

As seismic imaging is applied to more challenging situations where the overburden is ever more complex (e.g., imaging under complex and rugose salt bodies) and the illumination of important reflectors is spotty, the use of all the events in the data to generate interpretable images is important. Two classes of events that are often neglected, though they are also often present in complex data, are overturned reflections (Li et al., 1983) and prismatic reflections (Broto and Lailly, 2001). These two classes of events share the challenge that they cannot be imaged correctly (at least in laterally varying media) by downward-continuation migration methods. This obstacle can be overcome by reverse time migration (Baysal et al., 1983), and in particular by reverse time migration of shot profiles (Etgen, 1986).

The current status of reverse-time migration technology has some limitations that need to be addressed before it can be used effectively to image overturned and prismatic reflections. The main challenge is the extraction of useful and robust velocity updating information from the migrated image. In complex media, velocity is usually updated from the information provided by migrated Common Image Gathers (CIG). Filho (1992) presented the only other method published in the literature to compute angle-domain CIGs (ADCIGs) by reverse time migration. He applied the method to Amplitude Versus Angle (AVA) analysis. His method is computationally involved and it requires the identification of local plane waves.

In this paper, we extend to reverse-time shot-profile migration the method that Rickett and Sava (2001) proposed to compute CIGs by downward-continuation shot-profile migration. The idea is to compute offset-domain CIGs by a modified imaging condition that introduces the concept of a *subsurface offset*. Simple testing using synthetic data confirmed that CIGs computed by applying the proposed method can be used for velocity updating. They should also be useful for AVA analysis though we have not yet analyzed their amplitude properties. However, for both overturned reflections and prismatic reflections, the source wavefield and the receiver wavefield may be propagating along opposite vertical directions at the reflection point. For these two classes of events, the imaging principle can be generalized to include a *vertical subsurface offset* as well an horizontal one. Our real data example clearly shows the utility of this development.

The proper imaging of overturned waves is further challenged by the the need of discriminating between the image contributions of reflections generated from either side of an interface. These two reflections need to be separated both for imaging of reflectivity and for robust velocity updating. We present a simple generalization of the imaging condition that enables the determination of the propagation direction of the reflections, and thus the separation of the image contributions related to different events.

ANGLE-DOMAIN COMMON-IMAGE GATHERS

The conventional imaging condition for prestack reverse time migration is based on the crosscorrelation in time of the source wavefield (S) with the receiver wavefield (R). The equivalent of the stacked image is the average over sources (s) of the zero lag of this crosscorrelation; that is:

$$I(z,\mathbf{x}) = \sum_s \sum_t S_s(t,z,\mathbf{x})\, R_s(t,z,\mathbf{x}), \tag{1}$$

where z and $\mathbf{x}$ are respectively depth and the horizontal axes, and t is time. The result of this imaging condition is equivalent to stacking over offsets with Kirchhoff migration.

The imaging condition expressed in equation (1) has the substantial disadvantage of not providing prestack information that can be used for either velocity updates or amplitude analysis. The conventional way of overcoming this limitation is to avoid averaging over sources, and thus to create CIGs where the horizontal axis is related to a *surface offset*; that is, the distance between the source location and the image point. This kind of CIG is known to be prone to artifacts even when the migration velocity is correct because the non-specular reflections do not destructively interfere. Furthermore, in presence of migration velocity errors and structural dips, this kind of CIG does not provide useful information for improving the velocity field.

Rickett and Sava (2001) proposed a method for creating more useful angle-domain CIGs with shot profile migration using downward continuation. Their method is related to, but it is computationally more efficient than, the method introduced by de Bruin et al. (1990). It can be easily extended to reverse time migration by a generalization of equation (1) that crosscorrelates the wavefields shifted with respect to each other. The prestack image becomes function of the horizontal relative shift that has the physical meaning of a *subsurface offset* ($\mathbf{x}_h$). It can be computed as

$$I(z,\mathbf{x},\mathbf{x}_h) = \sum_s \sum_t S_s\left(t,z,\mathbf{x}+\frac{\mathbf{x}_h}{2}\right) R_s\left(t,z,\mathbf{x}-\frac{\mathbf{x}_h}{2}\right). \tag{2}$$

This imaging condition generates CIGs in the offset domain that can be easily transformed to the more useful angle domain by applying the same methodology described in (Sava et al., 2001).

Reverse time migration is more general than downward continuation migration because it allows events to propagate both upward and downward. Therefore the ADCIG computed from reverse time migration can be more general than the ones computed from downward-continuation migration. This more general imaging condition is needed when the source and receiver wavefields meet at a reflector while propagating along opposite vertical directions. This condition may occur either when imaging overturned

events or imaging prismatic reflections. We analyze these situations in more details in the following sections. To create useful ADCIGs in these situations we can introduce a *vertical offset* (z_h) into equation (2) and obtain

$$I(z,\mathbf{x},z_h,\mathbf{x}_h)=\sum_s\sum_t S_s\left(t,z+\frac{z_h}{2},\mathbf{x}+\frac{\mathbf{x}_h}{2}\right)R_s\left(t,z-\frac{z_h}{2},\mathbf{x}-\frac{\mathbf{x}_h}{2}\right). \tag{3}$$

These offset-domain CIGs should be amenable to being transformed into angle-domain CIG, by generalizing the methodology described in (Sava et al., 2001).

Examples of ADCIG to a simple synthetic data set

To illustrate the use of the proposed method to compute ADCIG we created a simple synthetic data set using a pseudo-spectral modeling code and then migrated the recorded shots using the same pseudo-spectral wave-propagation kernel. To avoid artifacts caused by reflections at the boundaries we used the one-way wave-equation boundary conditions presented in Shan (2002). We modeled and migrated 100 shots spaced 10 m apart. The receivers were in a symmetric split-spread configuration with maximum offset of 2,550 m. The model contained two reflectors: one dipping 10 degrees and the other flat. The dipping reflector is shallower than the flat one. The migration velocity was constant, and equal to the background velocity.

Figure 1 shows the CIGS obtained using the correct migration velocity. The panel on the left is the offset-domain CIG and the panel on the right is the angle-domain CIG. The CIGs are located at a surface location where both reflectors are illuminated well. As expected, the image is nicely focused at zero-offset in the panel on the left and the events are flat in the panel on the right.

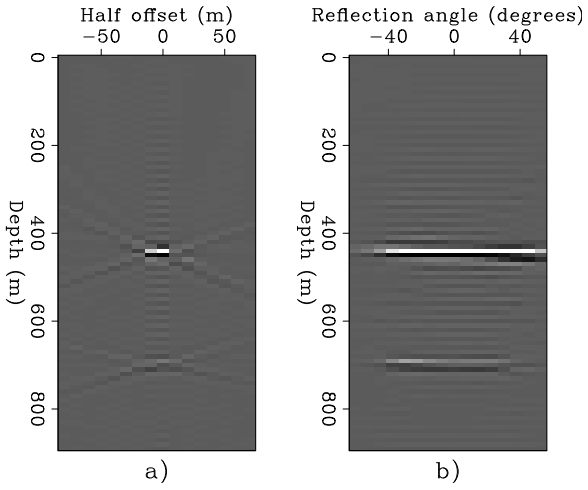

Figure 1: Offset-domain CIG (a) and angle-domain CIG (b) obtained using the correct migration velocity. Notice the focusing at zero offset in (a), and the flatness of the moveout in (b).

To illustrate the usefulness for velocity updating of the proposed method to compute ADCIGs, we have migrated the same data set with a lower velocity (.909 km/s). Figure 2 shows the CIGs obtained using the lower migration velocity. The panel on the left is the offset-domain CIG and the panel on the right is the angle-domain CIG. Both reflectors are undermigrated and shifted upward. Now in the panel on the left, the energy is not focused at zero offset, but it is spread over a hyperbolic trajectory centered at zero offset. The corresponding ADCIG (right) shows the characteristic smile typical of an undermigrated ADCIG (and some frowning artifacts). The velocity information contained in the panel on the right can be easily used for velocity updating and tomographic inversion in a similar fashion as the ADCIG obtained by downward-continuation migrations are used (Clapp and Biondi, 2000; Clapp, 2001).

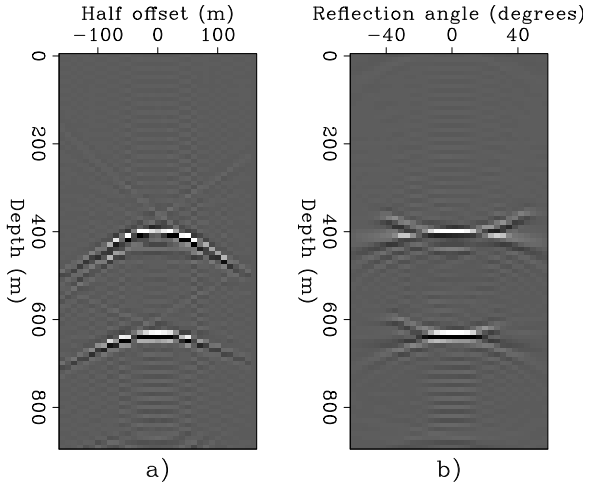

Figure 2: Offset-domain CIG (a) and angle-domain CIG (b) obtained using the lower migration velocity. Notice the lack of focusing at zero offset in (a), and the smile in (b).

PRESTACK IMAGES OF OVERTURNED REFLECTIONS

One of the main advantages of reverse-time migration methods over downward-continuation migration methods is their capability of imaging overturned events, even in presence of lateral velocity variations. However, this potential has not been exploited yet for prestack migration for several reasons. The computational cost is an important obstacle that is slowly being removed by progress in computer technology. In this section we will address two more fundamental problems. First, we need to discriminate between image contributions from reflections generated above an interface from the image contributions from reflections generated below the same interface. These two reflections have usually opposite polarities because they see the same impedance contrast from opposite directions. If their contributions to the image are simply stacked together, they would tend to attenuate each other. Second, we need to update the migration velocity from overturned reflections. Solving the first problem is crucial to the solution of the second one, as graphically illustrated in Figure 3. This figure shows the raypaths for both events. It is evident that the overturned event passes through an area of the velocity field different from the area traversed by the reflection from above. The information used for updating the velocity can thus be inconsistent for the two reflections, even showing errors with opposite signs.

The reflection from above and the reflection from below can be discriminated by a simple generalization of the imaging principle expressed in equation (3), that includes a time lag τ in the cross-correlation. In mathematical terms, we can generalize equation (3) as

$$I(z,x,h,\tau)=\sum_t S\left(t+\frac{\tau}{2},z+\frac{z_h}{2},x+\frac{h}{2}\right)R\left(t-\frac{\tau}{2},z-\frac{z_h}{2},x-\frac{h}{2}\right). \tag{4}$$

Now the image is function of an additional variable τ, that represents the correlation lag in time.

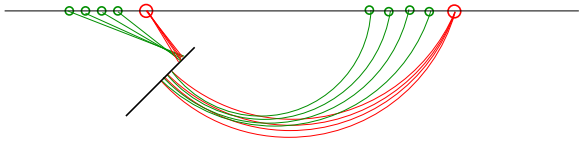

Figure 3: Ray paths corresponding to the reflection generated above the reflector and the one generated below the reflector. The rays corresponding to the source wavefield are red (dark in B&W), lines represent the wavefronts and the rays corresponding to the receiver wavefield are green. (light in B&W),

Examples of prestack imaging of overturned reflections

To illustrate the use of the proposed method to image overturned reflections we created a simple synthetic data set that contains such events. We immersed a thin high-velocity reflector in a layered medium with a strong vertical velocity gradient (.97 s^{-1}). The reflector is dipping 44 degrees with respect to the vertical and extends from a surface coordinate of 1 km to a surface coordinate of 1.35 km. We modeled and migrated 20 shots spaced 50 m apart, starting from the surface coordinate of 4.5 km. The receivers were in a symmetric split-spread configuration with maximum offset of 6.4 km. Because of the relative position of the reflector with respect to the shots, only the overturned reflections illuminate the reflector.

Figure 4 shows the image at $\tau = -.00525$ s (left) and the image at $\tau = .00525$ s (right). The dark lines superimposed onto the images show the position of the reflector in the model. In these two panels the reflector is almost as well focused as in in the image at $\tau = .0$ s (not shown here), but it is slightly shifted along its normal. As expected from the theoretical discussion above, the image of the reflector is slightly lower for the negative τ (left) than for the positive τ (right).

Figure 5 shows an example of CIG computed by evaluating equation (4) at $\tau = 0$. The panel on the left shows the offset-domain CIG, and the panel on the right shows the angle-domain CIG. The energy is correctly focused at zero offset in (a), and the event is flat in (b), though the angular coverage is narrow because of the short range of shot locations (1 km).

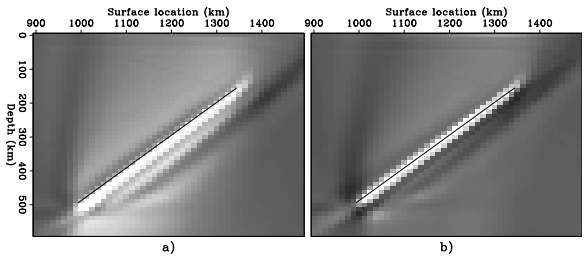

Figure 4: Images of the synthetic data set containing the overturned reflections migrated with the correct velocity; at $\tau = -dt/2$ (a) and at $\tau = dt/2$ (b) The dark segment superimposed onto the images shows the position of the reflector in the model. Notice the slight downward shift of the imaged reflector in (a) and the slight upward shift of the imaged reflector in (b).

NORTH SEA DATA EXAMPLE

We applied the method to a 2-D line of a North Sea data set that presents a difficult imaging problem caused by the interactions between the salt edge and a chalk layer. The analysis of the prestack

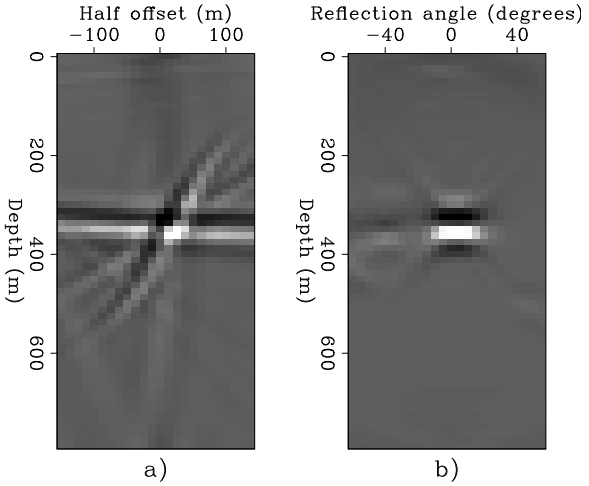

Figure 5: Offset-domain CIG (a) and angle-domain CIG (b) corresponding to the images in Figure 4. Notice the focusing at zero offset in (a), and the flatness of the moveout in (b), though the angular coverage is narrow because of the short range of shot locations (1 km).

data readily revealed the presence of overturned reflections, that are characterized by reverse moveouts in the CMP gathers. The migration velocity was determined by a tomographic inversion of ADCIGs obtained by downward-continuation prestack migration (Clapp and Biondi, 2000; Clapp, 2001). The velocity function is complex close to the salt edge, where a velocity inversion causes severe multipathing. Figure 6 compares the results obtained using an accurate downward-continuation prestack migration with the results obtained using reverse time migration. The downward-continuation migration does not image the vertical reflections because the source wavepath is overturned. On the contrary, the reverse time migration preserves those reflections, However, the focusing and the positioning of those overturned events is not accurate because of inaccuracies in the velocity model. The velocity model could be improved by inverting the information presents in the ADCIGs produced using the method introduced in this paper. Figure 7 shows three angle-domain CIGs located at surface location of 3.8 km (left), 4.8 m (center), and 5.8 km (right). Figure 8 shows the corresponding ADCIGs at the same surface locations. The ADCIG located away from the salt (3.8 km) is fairly flat, demonstrating that the velocity model is accurate for low-dip events. On the contrary, the ADCIG located exactly at the edge of the salt (4.8 km at a depth of about 2 km) is more difficult to interpret. It demonstrates the need of applying the more general imaging condition that included vertical subsurface offsets [equation (3)].

CONCLUSIONS

We presented a method to compute Common Image Gathers (CIG) from reverse-time shot profile migration. The proposed method generates accurate CIGs that can be used to update the migration velocity function, both for regular reflections and for overturned reflections.

The reflections generated from either side of an interface can be discriminated by computing the crosscorrelation of the source wavefield with the receiver wavefield at the non-zero time lag. This techniques is useful for imaging both overturned reflections and prismatic reflections.

The migration of a North Sea data set demonstrates the potential

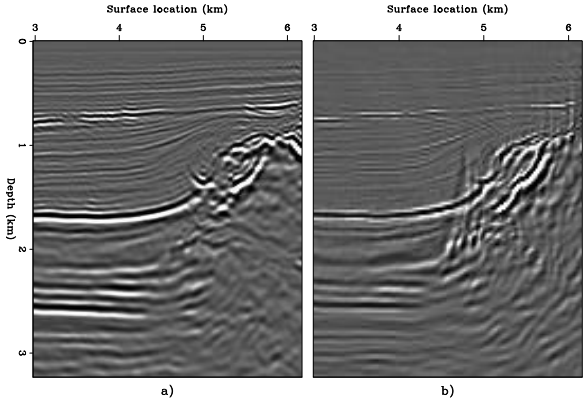

Figure 6: (a) Downward-continuation prestack migration, (b) reverse time prestack migration.

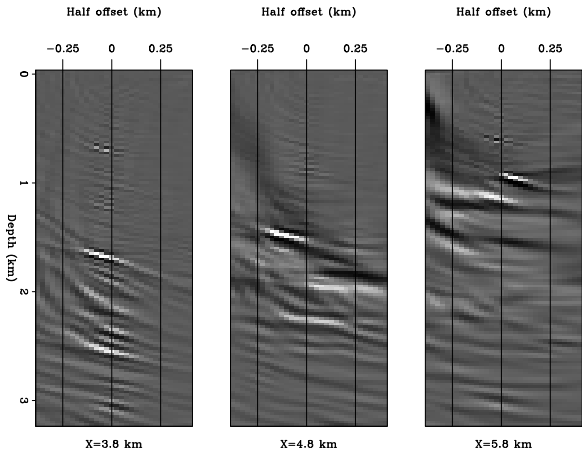

Figure 7: Offset-domain CIGs computed using equation (2).

of reverse time migration for imaging overturned reflections, and shows that overturned reflections are more sensitive to velocity errors than non-overturned reflections. The CIGs produced by the proposed method contain useful velocity information for updating the velocity model. However, the results suggest that we may need the computation of CIGs as a function of the vertical subsurface offset, in addition to the horizontal subsurface offset.

ACKNOWLEDGMENTS

We would like to thank TotalElfFina for making the North Sea data set available, and the sponsors of the Stanford Exploration Project for their financial support. We would like also to thank Robert Clapp for giving us the migration velocity model for the North Sea data set.

REFERENCES

Baysal, E., Kosloff, D. D., and Sherwood, J. W. C., 1983, Reverse time migration: Geophysics, **48**, no. 11, 1514–1524.

Broto, K., and Lailly, P., 2001, Towards the tomographic inversion of prismatic reflections: 71st Ann. Internat. Mtg., Soc. Expl. Geophys., Expanded Abstracts, 726–729.

Clapp, R., and Biondi, B., 2000, Tau domain migration velocity analysis using angle CRP gathers and geologic constrains: 70th Ann. Internat. Mtg., Soc. of Expl. Geophys., Expanded Abstracts, 926–929.

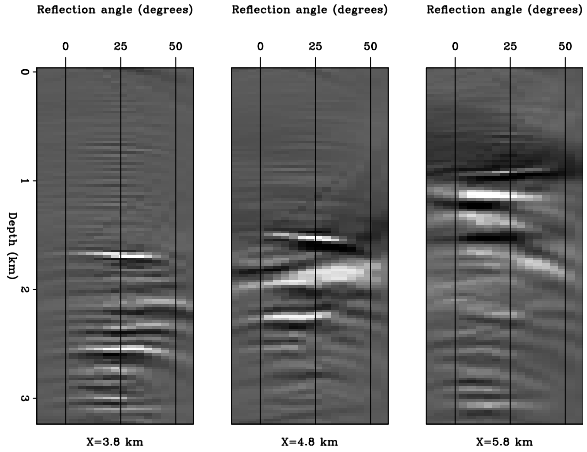

Figure 8: Angle-domain CIGs computed from the CIGS shown in Figure 7.

Clapp, R. G., 2001, Geologically constrained migration velocity analysis: Ph.D. thesis, Stanford University, `http://sep.stanford.edu/research/reports/theses.html`.

de Bruin, C. G. M., Wapenaar, C. P. A., and Berkhout, A. J., 1990, Angle-dependent reflectivity by means of prestack migration: Geophysics, **55**, no. 9, 1223–1234.

Etgen, J., 1986, Prestack reverse time migration of shot profiles: SEP–**50**, 151–170, `http://sep.stanford.edu/research/reports`.

Filho, C. A. C., 1992, Elastic modeling and migration in earth models: Ph.D. thesis, Stanford University.

Li, Z., Claerbout, J. F., and Ottolini, R., 1983, Overturned-wave migration by two-way extrapolation: SEP–**38**, 141–150, `http://sep.stanford.edu/research/reports`.

Rickett, J., and Sava, P., 2001, Offset and angle domain common-image gathers for shot-profile migration: 71st Ann. Internat. Meeting, Soc. Expl. Geophys., Expanded Abstracts, 1115–1118.

Sava, P., Biondi, B., and Fomel, S., 2001, Amplitude-preserved common image gathers by wave-equation migration: 71st Ann. Internat. Mtg., Soc. Expl. Geophys., Expanded Abstracts, 296–299.

Shan, G., 2002, One way wave equation absorbing boundary condition: SEP–**111**, 225–233, `http://sep.stanford.edu/research/reports`.